

# Assessing the Napo Karst Formation vulnerability in the Western Amazon River Basin

#### Elizabeth Naranjo

Universidad Regional Amazónica Ikiam

#### **Gabriel Massaine Moulatlet**

Instituto de Ecología, A.C

#### Ricardo Hirata

University of Sao Paulo (CEPAS-USP)

Bruno Conicelli ( bconicelli@gmail.com )

University of Sao Paulo (CEPAS-USP)

#### Research Article

Keywords: Amazon, DRASTIC, DRASTIC-LUC, EPIK, groundwater vulnerability, sensitivity analysis

Posted Date: August 2nd, 2023

**DOI:** https://doi.org/10.21203/rs.3.rs-3202914/v1

License: © (1) This work is licensed under a Creative Commons Attribution 4.0 International License. Read Full

License

#### **Abstract**

Karst environments are susceptible to contamination and directly affected by anthropogenic pressures. Remediation efforts are expensive, time-consuming, and often impractical. Hence, vulnerability maps can be valuable tools for protecting and preventing the aguifer's degradation. This study aims to evaluate the vulnerability of the Napo Karst Formation (NKF), in the western Amazon basin in Ecuador, using three vulnerability models: EPIK, DRASTIC, and DRASTIC-LUC. The difference between the three models lies in the parameters used and how each one of them address the vulnerability. Because assigning values to each parameter depends on the author's expertise and the available data, these models can produce varying outcomes, which we analyze using spatial and sensitivity analysis. Our results showed that DRASTIC and EPIK classified 45.76% and 35.38% of the NKF area as highly vulnerable, respectively, while DRASTIC-LUC classified most of the NKF areas under moderate vulnerability (57.47%). The sensitivity analysis determined that the depth to water table (D) and the infiltration conditions (I) were the most critical parameters for the vulnerability assessment. The moderate-to-high vulnerability of the NKF raises a warning, as the impacts on surface and groundwater may affect local populations that directly depend on its water. This is the first study that evaluates the vulnerability to the contamination of karst formation in the Ecuadorian Amazon. The results of this research can be used as a baseline for future research and as technical information for decision-makers to reduce the activities that could aggravate surface and groundwater quality in Western Amazonia.

#### 1. Introduction

Karstic aquifers are highly vulnerable to anthropogenic pressures (Tziritis and Lombardo 2017; Flores and Szucs 2022). Thin soil coverings, open recharge areas (dolines), shafts and shallow holes, and preferred flow paths in the epikarst and the vadose zone allow contaminants to easily reach groundwater and be transported promptly via karstic conduits and fractures over long distances (Zwahlen 2003; Tziritis and Lombardo 2017; Flores et al. 2020). The karst aquifer properties and the lack of paucity hydrogeological studies contribute to the false perception that karst water is pollution-free (Duarte et al. 2013; Jiménez-Madrid et al. 2019), but, the conversion of native vegetation and expansion of urban areas threaten aquifers, rendering karst settings especially susceptible to pollution in comparison to other hydrogeological habitats (Foster et al. 2002; Ravbar and Goldscheider 2009).

There is an incipient hydrogeological research development in Ecuador (Flores et al. 2020; Jiménez-Iñiguez et al. 2022; Campoverde-Muñoz et al. 2023; Intriago et al. 2023). Research efforts are concentrated in areas where groundwater is the primary source of water supply, such as the Andean and coastal regions (Espol Tech EP 2014; Calero et al. 2022; Intriago et al. 2023). For example, Quito's Public Water Supply Company (EPMAPS) promotes groundwater research for sustainable water supply, and geophysical prospecting surveys due to the increasing population in the Metropolitan District of Quito (Peñafiel et al. 2021). According to Flores and Szucs (2022), the low government entities' focus in groundwater research in the Amazon region could be attributed to their assumption that in this area there is a high rate of annual precipitation (2500-3000mm/year) (Villacís et al. 2008; INAMHI 2013), a low population, and relatively high-quality surface water for consumption.

In Ecuadorian Amazonia (the western portion of the Amazon basin), large karstic aquifers systems are present (Buckalew et al. 1998; Flores et al. 2020; Flores and Szucs 2022; Jiménez-Iñiguez et al. 2022). The high precipitation levels allow the karstification process to take place, giving rise to different structures that are representative of karst environments (Andreo et al. 2010; Stevanović 2015; Jiménez-Iñiguez et al. 2022). Previous

studies have focused on the geology, biodiversity, geobiodiversity, geoconservation, isotopic composition and speleological characteristics of the karst environment (Sánchez Cortez 2017; Constantin et al. 2018; Jiménez-Iñiguez et al. 2022; Sanchez-Cortez et al. 2022; Vera et al. 2023), but the vulnerability of karst environment is unknow.

The Amazon region has been exposed to environmental impacts caused by mining, extensive agriculture, fish farming, a lack of basic infrastructure and domestic waste, oil extraction (Lessmann et al. 2016), the mismanagement of solid waste in landfills, and the constant load of domestic waste outfall to the tributaries of major rivers (Capparelli et al. 2020, 2021; Galarza et al. 2022). For example, in the Napo River Basin, anthropogenic impacts are consequence of the growth of the population and the diversification of economic activities (Pimm et al. 2014; Capparelli et al. 2020). Studies suggest that anthropogenic activities have introduced metals and other contaminants into the aquatic systems in the Napo (Capparelli et al. 2020) and Aguarico rivers (Merchán and Chiogna 2017). This includes medium-scale to industrial-scale mining and oil exploration, emerging pollutants and microplastics that have impacted the quality of the aquatic ecosystems making water not recommended for human consumption (Cabrera et al. 2020, 2022; V. Capparelli et al. 2021; Galarza et al. 2022).

Because information on groundwater is relatively scarce in the Ecuadorian Amazonia and because aquifers are an important source of water for local population, groundwater vulnerability needs to be evaluated. Remediation efforts to polluted aquifers are expensive, time-consuming, and often impractical (Saidi et al. 2011; Hadžić et al. 2015; Dos Santos Filho et al. 2017; Terada et al. 2022). Then, the most reliable action is to prevent groundwater pollution (Aranda et al. 2019, 2021; Conicelli et al. 2021; Pileggi et al. 2021). For that purpose, there are useful tools, such as groundwater vulnerability assessments (GVA) are useful tools. GVA can consolidate highly complex technical information about hydrogeology and pollutants into a simple language that planners and decision-makers can use to plan and protect groundwater (Foster and Hirata 1988; Majandang and Sarapirome 2013; Baloch and Sahar 2014). For example, GVA of the aquifers that occur in Ecuador, such as those in the Limoncocha Biological Reserve (Jarrín et al. 2017); in Daule Aquifer (Ribeiro et al. 2017); in Gala, Tengel, and Siete River Basins, Ponce Enriquez mining area (Campoverde-Muñoz et al. 2023) have provided important information for the currently condition of these water bodies. However, there are no previous GVAs for karst environments.

Here, we use the available geographic information to model the vulnerability of the Napo Karst Formation in the western Ecuadorian Amazonia by using three models (DRASTIC, DRASTIC-LUC, and EPIK). We compare these models and discuss their qualities and problems in order to select the model that best suits the hydrogeological conditions of the study area. The protection of groundwater resources is imperative, especially in karst environments, such as Amazonia Karst (Pacheco et al. 2018; Jiménez-Iñiguez et al. 2022).

#### 2. Materials & Methods

Our methodology was designed to (1) collect data from relevant sources and prepare each parameter for each vulnerability model; (2) generate vulnerability maps using DRASTIC, DRASTIC-LUC, and EPIK; and (3) perform sensitivity analysis as an efficiency indicator.

# 2.1. Study Area

The Napo Formation is composed of three karst units, Napo North, Napo South, and Upano, formed by the combined runoff and slope of the calcareous rock structures (Flores and Szucs 2022). The area of Napo North and South henceforth referred to as the Napo Karst Formation (NKF) ranges between 2096 to 2971.41 km<sup>2</sup>. The karstic units present in the Amazon region form part of the so-called Amazon Karst System (AKS) (Chamba 2020) that covered around 4.5% of the Ecuadorian continental shelf (Flores and Szucs 2022). In conjunction with other units located in the coastal region of Ecuador (Fig. 1a), they are part of the karstic formations of South America.

Within the Ecuadorian territory, NKF is found mainly in the province of Napo and small parts of the provinces of Sucumbíos and Orellana (Fig. 1b). More than 70% of the NKF extension is located within protected areas: 28% are inside Sumaco Napo-Galeras National Park, 23% in the Cayambe-Coca Ecological Reserve, and 26% in the Napo-Sumaco Geopark (Fig. 1c). In the study area, the altitude ranges from 370 to 3039 m.a.s.l. The NKF is formed by limestone or karst caves (Chamba 2020) and, its lithology comprises black shales, limestone, and calcareous sandstones (Espol Tech EP 2014). The aquifers in the NKF can be local or discontinuous, shallow, with high flow velocity, and connected directly with the surface (Espol Tech EP 2014; Constantin et al. 2018). The NKF is poorly studied, probably due to the dense vegetation cover that makes accessibility to the area difficult (Chamba 2020).

# 2.2. Gathering and Evaluation of existing data

We collected geographic data from available repositories (Table 1), mainly those developed by government entities. Once the information was collected, it was processed with QGIS 3.12.0 (Fig. 2).

Table 1

Data sources to obtain the parameters of each methodology.

Data	Source
Land Use and Cover,  Protected Areas – Shapefile (1:100.000)	Ministry of the Environment, Water and Ecological Transition, Unique Environmental Information System (http://suia.ambiente.gob.ec)
Hydrogeologic, Soil, Geological, and Geopedological Data – Shapefile (1:100.000)	*MAGAP (http://geoportal.agricultura.gob.ec), National Information System (https://sni.gob.ec/coberturas)
STRM Worldwide Elevation Data - DEM (30 m)	United States Geological Survey (www.earthexplorer.com)
Monthly Precipitation Average (1970–2000) - Raster 30 sec (~ 1 km²)	WorldClim 2.1 (Fick and Hijmans 2017) (https://worldclim.org)
* Ministry of Agriculture, Livestock, Aquad	culture, and Fisheries

Missing values in the datasets were filled in with similar information from previous years, whenever available. This includes information on some parameters in protected areas. For example, missing data in the geopedological shapefiles were filled by merging information from the years 2016 and 2019, under the

assumption that both shapefiles contained the same variables. Other changes and adaptations made for the parameter determination are detailed below.

# 2.3. Groundwater Vulnerability Assessment

Because sources of environmental contamination are diffuse in Amazonia (Capparelli et al. 2020), we applied intrinsic vulnerability analysis, as this does not consider the source of the pollutants and their specific nature, but focuses on the natural environment's inherent geological, hydrological, and hydrogeological properties (Abiy et al. 2016). The intrinsic vulnerability analysis, we made using three models: to applied to any hydrogeological setting (DRASTIC and DRASTIC-LUC) and one specific to karstic environments (EPIK).

#### 2.3.1. DRASTIC Model

1

DRASTIC (Aller et al. 1987) is the most commonly model used for mapping groundwater vulnerability. It is calculated roughly analogous to the likelihood that pollutants released in a region reach the groundwater. That implies that high values are directly related to the probability of pollution (Shirazi et al. 2013; Talozi and Hijazi 2013). Vulnerability maps using DRASTIC have been applied to different environments and showed promising results in Algeria (Boufekane and Saighi 2018), Tunisia (Ayed et al. 2017), Bangladesh (Hasan et al. 2019), India (Khan and Jhariya 2019), Pakistan (Maqsoom et al. 2020), Nigeria (Oke 2020), Iran (Oroji and Karimi 2018), and England (Moustafa 2019). In Ecuador, Coello and Galárraga (2002) used the DRASTIC in the North Quito Aquifer to determine its susceptibility to pollution. DRASTIC assumes certain conditions, such as (1) pollutants are introduced through the soil, (2) precipitation carries pollutants into the groundwater, (3) pollutants move with the water, and (4) the assessment area is equal to or greater than 0.4 km² (Shirazi et al. 2013; Talozi and Hijazi 2013).

The acronyms of DRASTIC refer to seven hydrogeological parameters: (D) depth to groundwater, (N) net recharge, (A) aquifer media, (S) soil media, (T) topography, (I) impact on the vadose zone, and (C) hydraulic conductivity (Pathak et al. 2009). Eq. (1) describes how to calculate the DRASTIC index:

$$DrasticIndex = D_w \bullet D_r + R_w \bullet R_r + A_w \bullet A_r + S_w \bullet S_r + T_w \bullet T_r + I_w \bullet I_r + C_w \bullet C_r$$

Where, r and w are the rating and weight for each parameter, respectively (Table 2). To get a fair understanding of DRASTIC, each of DRASTIC parameters, its effect on aquifer vulnerability, and the ratings and weight it carries have been described in Table 2.

Table 2 Rating, ranges, and weight of each DRASTIC and DRASTIC-LUC parameters.

Thematic Layer	Parameter Symbol	Range	Rating	Parameter Symbol	Weight
Depth to Water Table (m)	$\mathrm{D_{r}}$	0-1.5	10	$\mathrm{D_w}$	5
		1.5-4.6	9		
Net Recharge (mm)	$R_{ m r}$	50-103	3	$R_{ m w}$	4
		103-178	6		
		178-254	8		
		> 254	9		
Aquifer Media	$A_{ m r}$	Sandstone, Limestone, and Shale sequence	6	$A_{ m w}$	3
Soil media	$S_{\mathrm{r}}$	Thin or Absent	10	$S_{\mathrm{w}}$	2
		Loamy sand	9		
		Loam	8		
		Sandy loamy	7		
		Silty loam	6		
		Clay loam	5		
		Sandy clay loam, Silty clay loam	4		
		Silty	3		
		Sandy clay, Silty clay	2		
		Clay, Heavy clay	1		
Topography (%)	$\mathrm{T_r}$	0-2	10	$\mathrm{T_w}$	1
		2.0-6.0	9		
		6.0-12.0	5		
		12.0-18.0	3		
		> 18.0	1		
Impact of Vadose Zone	$I_{\rm r}$	Shale	3	${ m I_w}$	5
		Limestone	6		

Thematic Layer	Parameter Symbol	Range	Rating	Parameter Symbol	Weight
Hydraulic Conductivity (mm/day)	$C_{ m r}$	0.04-4.8	1	$C_{ m w}$	3
		> 81.49	10		

The parameter *depth to the water table* is defined as the distance from the ground surface to the water table (Al-Zabet 2002). There is an inverse relationship between the depth of the water table and the pollution possibility, so, a deeper water table levels imply in less pollution (Zghibi et al. 2016; Kumar and Krishna 2020). Moreover, it is considered relevant to the depth of the material through which any pollutant travels before reaching the aquifer (Al-Zabet 2002). This parameter was obtained from the geopedological shapefile MAGAP (2015).

Net recharge indicates the amount of recharge that is positively correlated with the vulnerability rating (Saidi et al. 2010; Zghibi et al. 2016; Jang et al. 2017). Net recharge includes the average annual amount of infiltration without considering the distribution, intensity, or duration of recharge events (Al-Zabet 2002; Hirata and Conicelli 2012; Galvão et al. 2018; Conicelli et al. 2020; Intriago et al. 2023). Due to the lack of information for this parameter, the APLIS method (Andreo et al. 2004) was used to evaluate the mean annual recharge in carbonate aquifers (Zagana et al. 2011) as expressed as the percentage of precipitation that infiltrates into the soil. The APLIS method uses the following variables such as altitude (A), slope (P), lithology (L), infiltration (I), and soil (S). After the necessary process, the final map is calculated with Eq. (2):

$$\%Recharge = (A + P + 3 \bullet L + 2 \bullet I + S)/0.9$$

2

The APLIS method was developed for arid areas, so modifications and adaptations were necessary for this study (Table 3). The adaptations made were similarly to the study Duran et al (Durán et al. 2015), also done in the Amazon region, but in Peru. These adaptations were applied to lithology, infiltration, and soil according to Napo Formation conditions. For example, in preferential infiltration, we consider it necessary to consider geologic faults and caverns (mapped by Sánchez Cortez (2017), as preferential infiltration areas and give them a value of 10 while the rest of the regions acquire a value of 5, a similar approach used by Zagana et al. (2011) and Entezari et al. (2020). To obtain the recharge values it was necessary to use precipitation data. The available data was not useful because the precipitation values only covered accumulated data (1980–2010), and historical meteorological data from the stations network was incomplete. So, we used the average monthly rainfall (1970–2000) from WorldClim at scale of  $\sim$ 340 km². The recharge in mm is the result of a recharge factor (recharge%/100%) multiplied by the WorldClim precipitation raster for the area of interest.

Table 3
Range and rating of each parameter of the APLIS method used in this study, adapted from Andreo et al. (2004).

Altitude	(m)	Slope (%	6)	Lithology		Infiltration		Soil	
Range	Rating	Range	Rating	Range	Rating	Range	Rating	Range	Rating
300- 600	2	≤3	10	Limestones	7	Geologic faults	10	Andosols	10
900- 1200	4	16- 21	7	Shales	6	Caverns	10	Umbrisols	9
1500- 1800	6	31- 46	4	Sands, gravels	5	Rest	5	Leptosols	8
2100- 2400	8	>100	1	Granite, gneiss	4			Regosols	7
≥ 2700	10			Metamorphic and intrusive rocks	4			Cambisols	6
				Fine materials	3			Stagnosols	5
				Schists, slates	2			Gleysols	4
				Slimes, clays	2			Fluvisols	3
				Basalts, andesites	1				

The *aquifer media* indicates the rock material that serves as an aquifer inside the saturated zone (Saida et al. 2017), where the material properties control the pollutant attenuation processes (Awawdeh et al. 2015). This parameter is related to the permeability that is controlled by the geological characterization (Al-Zabet 2002; Zghibi et al. 2016). Thus, a high permeability allows more water and, therefore, more pollutants to enter the aquifer (Bhuvaneswaran and Ganesh 2019). The rating and range for this parameter were based on the hydrogeological shapefile (Table 1) and shown in Table 2.

The *soil media* parameter indicates the first zone that water, or any pollutant passes through when it percolates into the ground. For that reason, soil properties affect water transportation from the surface to the aquifer (Ouedraogo et al. 2016; Jang et al. 2017). Specifically, soil texture is the property that impacts the amount of recharge into the ground (Zghibi et al. 2016; Khosravi et al. 2018). This parameter was constructed using a geopedological and soil texture shapefile (MAGAP 2015). The soil order data was converted from the United States Department of Agriculture (USDA) taxonomy to the used by the World Reference Base (WRB).

The parameter *topography* determines the runoff and infiltration capacity of the water into the soil (Ouedraogo et al. 2016). Furthermore, it enables the collection of geographic information about pollutant concentration (Davis et al. 2002; Shirazi et al. 2013). The most important topographic parameter required is the slope, which was estimated from a DEM using GDAL tools available in QGIS. The range and rating for this parameter are the same as those used in the original methodology for DRASTIC.

Impact of the vadose zone. The vadose zone could be defined as the space between the water table and the ground surface (Shirazi et al. 2013; Jang et al. 2017). It is an essential parameter in the vulnerability assessment because it influences the residence time of the pollutants in the unsaturated zone (Shirazi et al. 2013; Ouedraogo et al. 2016). To estimate this parameter, the hydrogeological and geopedological shapefiles for the study area that contain a variable named lithology were used. Here, considering the information above, it was only necessary to place the value obtained from the original DRASTIC methodology.

Hydraulic conductivity is the capacity of an aquifer to allow fluids (water, pollutants) to pass through it and regulate their movement in the saturated zone (Al-Zabet 2002; Shirazi et al. 2013). Also, hydraulic conductivity is positively correlated with the vulnerability rating (Zghibi et al. 2016; Jang et al. 2017; Khosravi et al. 2018; Hasan et al. 2019). For this parameter, it is necessary to obtain aquifer data (transmissivity, grain size information, and thickness) to obtain the permeability, which is the same as the hydraulic conductivity, and that could be estimated from well data and pump tests. Nonetheless, when there is no information available, it is possible to use theoretical tables. Hydraulic conductivity values were assigned considering values by Freeze and Cherry (1979) for each lithology (derived from the geopedological and hydrogeological shapefile). The range and rating assigned are depicted in Table 2.

#### 2.3.2. DRASTIC-LUC Model

DRASTIC-LUC is a modified DRASTIC that includes Land Use and Cover. It is used to assess how human activities have impacted karstic and non-karstic areas (Umar et al. 2009). This model has primarily been used in India, with positive results (Alam et al. 2014; Sahoo et al. 2016; Kumar and Krishna 2020; Wei et al. 2021).

For the implementation in DRASTIC-LUC, "Land Use and Cover (LUC)" was defined as the cover over the soil and the activities therein. The water that has percolated through the soil, reaching an unsaturated zone, can also transport anthropogenic pollutants (Lerner and Harris 2009). Groundwater quality can be influenced by human actions. For example, inefficient wastewater treatment, agricultural activities, mining, and industrial tailings change the physical and chemical composition of water and increase its vulnerability (Ramaraju and Krishna Veni 2017). On the other hand, changes in land cover affect the available resources by changing recharge rates (Lerner and Harris 2009). A shapefile with information about land use and cover from 2018 was considered for the study area. Eq. (3) shows how DRASTIC-LUC is calculated.

$$DRASTIC - LUC = DrasticIndex + LUC_r \bullet LUC_w$$

3

Where the subscripts r and w are the rating and weight for each parameter, respectively. DRASTIC-LUC assigned a low value to natural areas (forests) and high values to agricultural, urban, and water bodies. The values assigned are shown in Table 4 and their distribution is in Fig. 1c.

Table 4
Rating, ranges, and weight for LUC parameter inside of DRASTIC-LUC index.

Parameter	Symbol	Range	Area %	Rating	Symbol	Weight
Land Use and Cover		Native Forest, Herbaceous Vegetation	78.91	3	$\mathrm{LU}_{\mathrm{w}}$	5
	$\mathrm{LU}_r$	Built-Up Land	0.18	5		
		Populated Area, Agricultural Land	20.62	7		
		Water Bodies	0.28	9		

#### 2.3.3. EPIK Model

Intrinsic vulnerability assessment in karst areas requires a model that considers geomorphological, hydrological, and hydrogeological characteristics (Gogu and Dassargues 2000; de Castro and Menegasse 2017). The EPIK model was chosen because it is one of the most widely used models for vulnerability assessment that is specific to karst environments (Hammouri and El-Naqa 2008). EPIK was developed by Doerfliger and Zwahlen (1998). It is an acronym for epikarst (E), protective cover (P), infiltration conditions (I), and karst network development (K).

A multi-attribute weighting-rating model (Doerfliger et al. 1999) analyzes four parameters individually and combines them using a raster calculator (Doummar et al. 2012). Also, this model has been applied in different environments such as Brazil (Lenhare and Sallun Filho 2019; Pereira et al. 2019), Algeria (Nekkoub et al. 2020), Morocco (Alili et al. 2018), Greece (Vogelbacher et al. 2019). The final product is the protection factor (F). A low F value represents high vulnerability, while a high F value shows low vulnerability (Marín and Andreo 2015). The index is calculated as follows:

$$F_i = (\propto \bullet E_i) + (\beta \bullet P_i) + (\gamma \bullet I_i) + (\delta \bullet K_i)$$

4

Where,  $F_i$  is the protection factor for each subarea i;  $\alpha$ ,  $\beta$ ,  $\gamma$ , and  $\delta$  are the weighting factor for each parameter E, P, I, and K. Table 5 contains the value assigned for the weighting as mentioned earlier and the rating for each parameter. The ratings for each class of a given attribute are multiplied by the weight related to the point, and then the products are added up to arrive at a final score (Doerfliger et al. 1999).

Table 5
Values for each EPIK parameter were obtained from Doerfliger and Zwahlen (1998).

Parameter	Symbol	Range	Rating	Symbol	Weight
Epikarst	E <sub>1</sub>	Sinkholes or dolines, karren, polje, caves, springs	1	$\propto$	3
	E <sub>2</sub>	Intermediate zones along doline alignments	2		
Protective Cover	P <sub>2</sub>	20-100 cm of soil with low hydraulic conductivity	2	β	2
	P <sub>3</sub>	> 1 m of soil with low hydraulic conductivity	3		
Infiltration Conditions	l <sub>2</sub>	The slope is more than 10% for cultivated areas and less than 25% for meadows and pastures	1	$\gamma$	1
	l <sub>3</sub>	The slope is less than 10% for cultivated areas and less than 25% for meadows and pastures	2		
Karst Network	K <sub>1</sub>	Well-developed karstic network with little fill and well-interconnected conduits	1	δ	3
	K <sub>2</sub>	Poorly karstic network with poorly interconnected or infilled drains or conduits	2		

*Epikarst* is the karstified zone under the soil cover. In some areas, this is open to the surface (Doummar et al. 2012; Stevanović 2015; Bakalowicz 2019). Furthermore, it controls the infiltration into the aquifer and stores water (Goldscheider 2005). The geomorphological information available (SIGTIERRAS 2015) and the speleological information of the Napo province (Sánchez Cortez 2017) were used to determine this parameter. Here, areas around 500 m from the caves and karst morphologies were identified as  $E_1$  and the rest of the study area as  $E_2$  (Table 5).

The protective cover is defined by soil cover, deposits, and lithologic or non-karstic geological formations over the aquifer (Doummar et al. 2012; Nekkoub et al. 2020). It is one of the natural protection parameters generally accounted for in vulnerability mapping (Doerfliger and Zwahlen 1998). To estimate this parameter, soil and a geopedological shapefile with detailed information were considered. In particular, the geopedological shapefile contains categories associated with soil depth that allow one to establish the weight for this parameter.

Infiltration conditions are complex to estimate (Gogu and Dassargues 2000) because they determine how aquifer recharge occurs (Doerfliger and Zwahlen 1998). Infiltration conditions can be estimated using the slope percentage and a land cover shapefile (Hurtado-Pidal et al. 2022). A correlation between these variables allows assigning the rating values according to the original methodology for EPIK.

Karst network refers to the degree of karstification or the dissolution process of soluble rocks (limestone, dolomites, gypsum) by physiochemical interaction with water (Barea et al. 2002; Doummar et al. 2012). This parameter can be determined through direct geomorphological identification, tracer tests, or variability in water quality (Nekkoub et al. 2020). Nevertheless, no field trips could be carried out to identify and register the karst network. For that reason, geomorphological (SIGTIERRAS 2015), speleological (Sánchez Cortez 2017), and other related data were employed to assign a value to this parameter. Areas with geomorphological characteristics of a

karst environment and the presence of caves were assigned as  $K_1$  under the assumption that the karst network beneath the caves was well developed and the rest of the area was assigned as  $K_2$ .

### 2.4. Categorization Scale

The fact that each methodology is different makes it difficult to compare the areas corresponding to each level of vulnerability. So, for comparative purposes, we standardized the scale for all vulnerability indices as drawn for the three models, so it, ranges from 0 to 1:

$$X_i = (X-min)/(max-min)$$

5

Where,  $X_i$  is the value derived from the new scale, X is the original value obtained from each vulnerability index, min and max are the minimum and maximum values of the vulnerability index, respectively. To visually identify vulnerability, 5 ranges of vulnerability classes were established, and each was assigned a specific color, Table 6.

**Table 6.** Vulnerability classes from Aller et al. (1987), Doerfliger and Zwahlen (1998), and the new scale for each index.

Class	Color	Rango DRASTIC / DRASTIC-LUC	Rango EPIK	New Classes	Color	Range
Low		65 - 105	$> 25 \text{ con } P_4 + I_{3,4}$	Very Low		0.0 - 0.2
Moderate		105 - 146	> 25	Low		0.2 - 0.4
High		146 - 187	20 - 25	Moderate		0.4 - 0.6
Very High		187 - 230	9 - 19	High		0.6 - 0.8
				Very High		0.8 - 1.0

# 2.5. Sensitivity Analysis

Sensitivity analysis considers the contribution of individual factors and entry parameters to the outcome of an analytical model (Napolitano and Fabbri 1996). It means that estimating changes in the output map by changing the input parameters helps to understand the effect of the parameters on the output of the model (Thapa et al. 2018). Two types of sensitivity analyses (Single Parameter Sensitivity and Map Removal Sensitivity) were used for this study. These analysis have been used to evaluate the reliability of vulnerability criteria and validate developed vulnerability maps (Tomer et al. 2019).

# 2.5.1. Single Parameter Sensitivity Analysis

The single parameter sensitivity analysis, or weighting factor (Napolitano and Fabbri 1996), determines the impact of each parameter within the vulnerability index. The effective weight of each parameter is calculated by using the following equation:

$$W_{xi} = \left(P_{ri} \bullet P_{wi}\right)/V_i \bullet 100\%$$

Where,  $P_{ri}$  is the rating of each parameter,  $P_{wi}$  is the weight corresponding to each parameter, and  $V_i$  as the vulnerability index. The mean percent error (MPE) shows the increase or decrease of the effective weight compared with the theoretical value. It is calculated with the following equation:

$$MPE = \left( \left| Theoretical - Real \, \right| \right) / Theoretical ullet 100\%$$

7

# 2.5.2. Map Removal Sensitivity Analysis

This sensitivity analysis was developed by Lodwick et al., (1990) and describes the sensitivity of the vulnerability index when removing one or more parameters from the suitability analysis. It is computed with the equation:

$$S = \left( \left| V_i / N - V_{xi} / n \right| \right) / V_i \bullet 100\%$$

8

Where  $V_i$  is the vulnerability index, N is the number of layers used for computing  $V_i$ ,  $V_{xi}$  is the vulnerability index excluding one layer and n is the number of layers used for calculating  $V_{xi}$ .

Both sensitivity analyses have been used to analyze the reliability of vulnerability criteria (Tomer et al. 2019). Applying these vulnerability indices may be subjective as the result depends on the author's weighting assigned to each parameter. Therefore, sensitivity analysis provided useful information on the effects of weight and rating values applied to each parameter and allowed determining the importance of the subjective aspects (Gogu and Dassargues 2000).

#### 3. Results and Discussion

# 3.1. Vulnerability Models

DRASTIC index values were between 102 and 190, while for DRASTIC-LUC, the values were between 117 and 230. For the EPIK model, the values were between 13 and 22 (Table 7). Figure 3 shows the adjusted color-coded vulnerability maps and the area under each vulnerability class. The DRASTIC model showed that about 45.76% (959.40 km²) of the study area had high vulnerability, followed by 22.51% (471.96 km²) of low exposure, and a small percentage pertains to very high vulnerability (1.06%) (Table 8). In contrast, the DRASTIC-LUC showed that 57.47% (1204.72 km²) had moderate vulnerability, while 23.10% (484.23 km²) of the area was classified as low vulnerable, and 0.81% as very highly vulnerable (Table 8). Compared to the other indices, the EPIK model showed a similar distribution for low to high vulnerability, so that 35.38% of the mapped area (741.78 km²) had high vulnerability, followed by 25.72% (539.29 km²) as low vulnerable, and 24.24% (508.14 km²) as moderate vulnerable (Table 8). The percentage of very highly vulnerable area was low (5.60%). This pattern of low percentages was similar to the very low vulnerability with low values.

Table 7 Statistics of the initial index.

Vulnerability Index	Mean	Min	Max	SD		
DRASTIC	157.21	102	190	18.27		
DRASTIC-LUC	165.45	117	230	17.09		
EPIK	17.6	13	22	2.06		
Min = Minimun, Max = Maximun, SD = Standard Deviation						

Table 8

Area distribution, in percentage and km<sup>2</sup>, for each initial index.

Vulnerability Class	DRASTIC DRASTIC-LUC EPIK		DRASTIC-LUC			
	(%)	(km²)	(%)	(km²)	(%)	(km²)
Very Low	10.67	223.75	13.21	276.90	9.05	189.72
Low	22.51	471.92	23.10	484.23	25.72	539.29
Moderate	19.99	419.07	57.47	1204.72	24.24	508.14
High	45.76	959.40	5.42	113.66	35.38	741.78
Very High	1.06	22.25	0.81	16.89	5.60	117.47

# 3.2. Sensitivity Analysis

Table 9 summarizes the statistics of all parameters and their resulting weights employed in each vulnerability index. By analyzing the mean value of the weight that DRASTIC (Table 2) assigned to each parameter, the parameter depth of the water table (9.02) appeared as the most critical contributor. In the case of EPIK (Table 5), the infiltration conditions (2.86) appeared to be the most critical contributor to the model. On the contrary, topography (2.87) and karst network (1.25), contribute the least to DRASTIC/DRASTIC-LUC, and EPIK, respectively.

Table 9
Statistical summary of each model parameter.

Parameters	Symbol	Mean	Min	Max	SD
Depth to the water table	D	9.02	9	10	0.14
Net <b>R</b> echarge	R	5.76	1	8	1.32
<b>A</b> quifer media	А	6.00	6	6	0.00
Soil media	S	5.58	1	10	2.12
Topography	Т	2.87	1	10	2.51
Impact of the vadose zone	I	4.98	3	6	1.42
Hydraulic <b>C</b> onductivity	С	6.93	1	10	4.27
Land and Use Cover	LUC	3.98	3	9	1.99
<b>E</b> pikarst	Е	1.37	1	2	0.48
Protective cover	Р	2.43	2	3	0.50
Infiltration conditions	I	2.86	2	3	0.35
<b>K</b> arst network	K	1.25	1	2	0.43

# 3.2.1. Single Parameter Sensitivity Analysis

In this analysis, we use the theoretical weight as a value and percentage that comes from each vulnerability model, and we calculate an effective weight that depends on the theoretical weight and the resulting vulnerability. The contribution of each parameter was directly related to its weight in the final vulnerability calculation. For the DRASTIC model, our analysis of the effective weighting (Table 10) indicates that parameter D dominates the vulnerability index, and that D becomes the most influential, with an effective weight of 7.25 (31.52%). This might be because the weight and the values assigned to parameter D for the study area corresponded to the shallow water table (less than 5m depth). Also, it could relate to parameter vadose zone thickness (parameter I) because if the water table is closer to the surface, it means that the vadose zone is smaller in size. Thus, any pollutant load would be more easily introduced into the groundwater, generating major contamination problems. Even though, parameter I decreased from 5 (21.74%) to 3.84 (16.71%), with a lower error percentage (Table 10). In the case of the parameter T, our results showed that the weight drastically reduces its value (1 to 0.46), causing the error percent to be high (53.56%) and indicating that the slope is not significant and the least contributor to the vulnerability calculation. This contrasts with the study by Kumar and Krishna (2020). Their results show that parameter C is the least important contributor to the index, and the depth to the water table (D) and vadose zone thickness (I) contribute more to the vulnerability index after the effective weighting factor, which contrasts with our results, where only the parameter D is the major contributor to the index.

Table 10 Statistics of single parameter sensitivity analysis for each vulnerability index.

Parameter	Theoretical Weight	Theoretical Weight (%)	Effectiv	ve Weight	: (%)		Real Weight	Mean Error %
	Weight	(%)	Mean	Min	Max	SD	weight	шог ж
D	5	21.74	31.52	24.32	44.25	4.29	7.25	44.99
R	4	17.39	16.13	2.70	27.59	4.38	3.71	7.25
А	3	13.04	12.58	9.47	17.65	1.70	2.89	3.53
S	2	8.70	7.72	1.23	16.81	3.09	1.77	11.26
Т	1	4.35	2.02	0.55	8.55	1.85	0.46	53.56
I	5	21.74	16.71	10.14	22.39	3.38	3.84	23.14
С	3	13.04	13.31	2.03	22.39	7.96	3.06	2.07
D	5	17.86	27.57	20.27	39.06	3.10	7.72	54.37
R	4	14.29	14.07	2.27	24.43	3.53	3.94	1.54
А	3	10.71	11.01	7.826	15.38	1.23	3.08	2.75
S	2	7.14	6.74	1.00	14.93	2.60	1.89	5.60
Т	1	3.57	1.74	0.45	7.58	1.55	0.49	51.26
1	5	17.86	14.82	7.77	20.13	3.55	4.15	17.02
С	3	10.71	12.00	1.55	20.13	7.31	3.36	12.02
LUC	5	17.86	12.06	7.32	29.41	5.83	3.38	32.47
Е	3	33.33	22.10	15.79	37.50	6.64	1.99	33.69
Р	1	11.11	14.26	9.52	21.43	2.95	1.28	28.35
1	3	33.33	47.22	31.58	56.25	6.15	4.25	41.67
K	2	22.22	16.43	10.00	26.67	5.16	1.48	26.06

Similarly to the DRASTIC, for the DRASTIC-LUC, the effective weight calculated for the parameters D, A, and C increased to 7.72 (27.57%), 3.08 (11.01%), and 3.36 (12.00%), respectively. In addition, parameter R showed a decline from 4 (10.71%) to 3.94 (14.07%). Regarding the parameter LUC, it had a weight equal to 5 (17.86%) in the index calculation, which means that LUC had a detrimental impact on vulnerability. Nevertheless, with the real weight, this value decreased to 3.38 (12.06%). This could be related to the fact that the LUC parameter did not have a great influence on the increase in vulnerability because most of the study area is still covered by natural areas. This contrasts with the assignment given to the LUC parameter by Kumar and Krishna (2020), in an area with a predominance of agriculture and coal mining activities and with a small proportion of natural areas. In their case, LUC had a significant influence on the DRASTIC-LUC model. In the Napo province, the extent of the pollution generated by agricultural activities is still not mapped, although it has been shown that pollution can spread dozens of kilometers from the main sources (Capparelli et al. 2020; Galarza et al. 2021; Lucas-Solis et al.

2021). Therefore, it would be necessary to consider a more in-depth mapping of land use and cover in NKF to generate more realistic results for the study area.

For the EPIK model, the value of the parameter E declined from 3 to 1.99 when the effective weight factor was calculated. Parameter K experiences a similar decline from 2 to 1.8. These results indicate that the impact on the vulnerability index of parameters E and K was lower than the other parameters (P and I). This could be related to the criteria and the information that was used to obtain the E and K parameters. In the absence of explicit information on the karstic network and epikarst, assumptions were made based on available information and previous knowledge. On the other hand, for the parameter I the theoretical value was 3 (33.33%), and the updated value was 4.25 (47.22%), while in the case of P, the weight changed from 1 (11.11%) to 1.28 (14.26%). The parameter P presented a slight increase that could be related to the soil thickness above the water table that is close to the surface. On the other hand, the considerable increase in the P parameter could also be associated with the fact that the study area is in a foothill zone where the slope in the lower zone is less than 25%, facilitating the infiltration of water and possible pollutants. These results contrast to the ones obtained by the DRASTIC model, where the slope (parameter T) was found to be unimportant for vulnerability calculation and thus had low weight.

Once the effective weight or the real weight had been determined, each vulnerability index was recalculated. The actual weight obtained from the effective weight produces a variation in each vulnerability class's area. This shows somehow more realistic results with the characteristics of the study area and the ranges and ratings employed. As summarized in Table 11, changes occurred in the statistics of each model, meaning an increase or decrease in the values compared to the originals. Regarding the reclassification of vulnerability maps (Fig. 4), for DRASTIC, the area of high vulnerability slightly increased (from 45.76–48.95%) compared to moderate vulnerability (from 19.99–15.21%). Also, the values for very low and very high vulnerability increased to a lesser degree (from 10.67–12.11% and from 1.06–1.22%, respectively). For DRASTIC-LUC, the values of moderate vulnerability (from 57.47–48.09%) were reduced to a greater extent than for the other classes. However, for high vulnerability, the value increased from 5.42–16.59%. For the EPIK model, the percentage of highly vulnerable areas increased from 35.38–47.98%, and similarly, the percentage of very highly vulnerable areas went from 5.60–17.15%. By contrast, moderate, low, and very low vulnerable areas decreased. It is especially noteworthy that low vulnerability has decreased from 25.72–5.91% (Fig. 5).

Table 11
Statistics of the initial index and the index after weighting factor (WF).

Vulnerability Index	Mean	Min	Max	SD
WF_DRASTIC	155.26	115.5	195.8	17.26
WF_DRASTIC-LUC	179.77	133.6	236.6	17.26
WF_EPIK	19.82	14.53	23.53	2.05
DRASTIC	157.21	102	190	18.27
DRASTIC-LUC	165.45	117	230	17.09
EPIK	17.6	13	22	2.06

# 3.2.2. Map Removal Sensitivity Analysis

The values corresponding to the variation index showed that leaving-one-out of the parameter causes a variation in the resulting vulnerability index (Table 12). When analyzing the DRASTIC and DRASTIC-LUC statistical data, they followed a similar pattern, D > T > C > S > LUC > I > R > A, without the LUC parameter for DRASTIC. For DRASTIC, the parameters causing the least variation were A (0.35%), R (0.61%), and I (0.64%), while for DRASTIC-LUC, they were A (0.25%), R (0.45%), I (0.56%) and LUC (0.68%). Interestingly, these parameters produced the least variation considering their weight within the index calculation (Table 2 and Table 4). On the other hand, for EPIK, the parameter that produced the least variation was E (2.13%), which contrasts with parameter I (7.97%), which was responsible for the greatest variation. The pattern of variation obtained from this model was I > P > K > E.

Table 12
Statistics of map removal sensitivity analysis: one parameter removed.

Parameter Removed	Variation index (%)					
	Mean	Min	Max	SD		
Depth to the water table	2.87	1.67	4.99	0.71		
Topography	2.04	0.96	2.29	0.31		
Hydraulic <b>C</b> onductivity	1.21	0.25	2.04	0.57		
Soil media	1.10	0.00	2.18	0.51		
Impact of the vadose zone	0.64	0.02	1.35	0.27		
Net Recharge	0.61	0.00	2.20	0.50		
<b>A</b> quifer media	0.35	0.00	0.80	0.19		
<b>D</b> epth to the water table	2.15	1.11	3.79	0.44		
Topography	1.54	0.70	1.72	0.22		
Hydraulic <b>C</b> onductivity	0.97	0.08	1.56	0.40		
Soil media	0.82	0.01	1.64	0.37		
Land and Use Cover	0.68	0.01	2.42	0.48		
Impact of the vadose zone	0.56	0.01	1.09	0.22		
Net Recharge	0.45	0.00	1.70	0.32		
<b>A</b> quifer media	0.25	0.00	0.67	0.11		
Infiltration conditions	7.97	2.19	10.42	1.83		
Protective cover	3.69	1.19	5.16	0.96		
<b>K</b> arst network	3.63	0.00	5.00	1.43		
<b>E</b> pikarst	2.13	0.64	4.17	0.68		

The resulting patterns in Table 12 allowed for a new exclusion analysis where more parameters were eliminated until only the one that generated the most variation remains. The variation index after removing more parameters is shown in Table 13. The models may agree on the same level of vulnerability in some areas while disagreeing in other areas. The notable difference may be related to the number of parameters considered by each methodology. For example, DRASTIC is based on seven hydrogeological parameters that are combined to assess vulnerability. DRASTIC-LUC includes the parameters mentioned above, plus land use and cover related to anthropogenic activities. In contrast, EPIK only consists of four parameters oriented to specific characteristics of karst environments that require a higher level of information and specificity. According to Hammouri and El-Naqa (2008), the capacity of EPIK to characterize epikarstic features is an essential distinction between it and DRASTIC when the area to be evaluated presents epikarstic traits.

Table 13
Statistics of map removal sensitivity analysis. The variation index caused after using only one parameter o many of them to calculate the vulnerability index.

Parameter Used						Variation index (%)						
							Mean	Min	Max	SD		
DRASTIC												
D	Т	С	S	I	R		0.45	0.00	0.83	0.24		
D	Т	С	S	I			0.36	0.00	1.37	0.33		
D	Т	С	S				1.87	0.00	4.79	1.56		
D	Т	С					3.57	0.06	9.59	2.63		
D	Т						1.86	0.00	8.10	1.87		
D							14.84	9.52	27.73	3.78		
DRASTIC-LUC												
D	Т	С	S	LUC	I	R	0.25	0.00	0.67	0.11		
D	Т	С	S	LUC	I		0.53	0.00	2.19	0.45		
D	Т	С	S	LUC			0.66	0.00	2.42	0.39		
D	Т	С	S				0.89	0.00	4.33	0.87		
D	Т	С					1.88	0.00	5.37	0.98		
D	Т						2.20	0.00	9.40	1.78		
D							15.07	7.77	26.56	3.10		
EPIK												
I	Р	K					2.13	0.64	4.17	0.68		
I	Р						6.48	0.00	10.29	3.03		
I							23.91	6.58	31.25	5.48		

There was no direct association between the number of removed parameters and the variation in the vulnerability index. The findings of Kumar and Krishna (2020), which used DRASTIC and DRASTIC-LUC, show a different pattern on the parameters causing the least variation (I > D > C > LUC > S > T > R > A). In their study, the factor that exhibited the most variation was the impact on the vadose zone (parameter I), which weighed 5. In other words, the variations were directly associated with values assigned to each parameter and their weight in the calculation. Nonetheless, it is unfeasible to evaluate vulnerability using one or three parameters because inconsistent values can be obtained and do not reflect the reality of the study area.

When contrasted to DRASTIC or DRASTIC-LUC, EPIK employs just four parameters with a limited range of values and weights. Therefore, removing one or more parameters creates a significant variation in the final output. For example, eliminating parameter I causes more variation than removing parameter E. Nevertheless, the infiltration conditions are intriguing because they have a low vulnerability index weight but produce the highest variation when removed. That could be related to how the protective factor operates, where low values represent high vulnerability and high values represent low vulnerability (Doerfliger and Zwahlen 1998; Doerfliger et al. 1999).

#### 4. Conclusion and Recommendations

The first step in the protection of groundwater resources is the vulnerability assessment, which is carried out in this research. Then the potential contamination sources are mapped, so that using these two pieces of information, we will obtain a complete overview of the most vulnerable areas and the potential sources of contamination risk. The use of vulnerability maps becomes important and necessary when there are contamination sources on the surface that could threaten groundwater quality. Even more so in a karst environment, already considered vulnerable, and located in the Amazon region that has been exploited for its biodiversity and has received a slight investment in development in return.

It is important to emphasize that this is the first research that evaluates the vulnerability of karst formation in the Ecuadorian Amazon. Our research used DRASTIC, DRASTIC, and EPIK to evaluate the vulnerability of the Napo Karst Formation (NKF). Our results showed that DRASTIC and EPIK, classify 45.76% and 35.38% of the NKF as highly vulnerable, respectively, while DRASTIC-LUC shows moderate vulnerability (57.47%). The sensitivity analysis showed that the weight assigned to each parameter affects the final vulnerability index, and for the NKF the most critical parameter is the Depth to water table (D). The moderate-to-high vulnerability of the NKF raises a warning, as the impacts on surface and groundwater may affect local populations that directly depend on its water. Therefore, the results obtained can be used as a baseline for future research and as technical information for decision-makers to reduce the activities that could aggravate surface and groundwater quality in Western Amazonia. There is evidence of contamination problems at the surface, and due to the interaction between the surface and groundwater, this resource may be in potential danger if the appropriate actions are not taken.

#### **Declarations**

Funding: No funds, grants, or other support was received.

**Data Availability:** The data generated and analyzed are shown in this manuscript. Details of how the data were obtained and processed are given in the methodology section. No secondary data was generated that should be stored in a repository.

**Conflict Interests:** The authors declare no competing financial interests or personal relationships that could have appeared to influence the work reported in this paper.

Author's Contribution: Conceptualization: Bruno Conicelli; Methodology: Elizabeth Naranjo, Bruno Conicelli; Formal analysis, investigation, and data curation: Elizabeth Naranjo, Gabriel Massaine Moulatlet, Ricardo Hirata; Writing - original draft preparation: Elizabeth Naranjo, Bruno Conicelli; Writing - review and editing: Gabriel Massaine Moulatlet, Ricardo Hirata; Supervision and project administrator: Bruno Conicelli. All authors reviewed the manuscript and approved it for publication.

#### References

- 1. Abiy AZ, Melesse AM, Behabtu YM, Abebe B (2016) Groundwater vulnerability analysis of the tana sub-basin: An application of drastic index method. In: Melesse AM, Abtew W (eds) Landscape Dynamics, Soils and Hydrological Processes in Varied Climates, Springer Geography. pp 435–461
- 2. Al-Zabet T (2002) Evaluation of aquifer vulnerability to contamination potential using the DRASTIC method. Environ Geol 43:203–208. https://doi.org/10.1007/s00254-002-0645-5
- 3. Alam F, Umar R, Ahmed S, Dar FA (2014) A new model (DRASTIC-LU) for evaluating groundwater vulnerability in parts of central Ganga Plain, India. Arab J Geosci 7:927–937. https://doi.org/10.1007/s12517-012-0796-y
- 4. Alili L, Boukdir A, Maslouhi MR, Ikhmerdi H (2018) Karst groundwater vulnerability mapping to the pollution: Case of Dir springs located between EL KSIBA and Ouaoumana (High Atlas, Morocco). E3S Web Conf 37:1–11. https://doi.org/10.1051/e3sconf/20183701004
- 5. Aller L, Bennett T, Lehr JH, et al (1987) DRASTIC: A Standardized Method for Evaluating Ground Water Pollution Potential Using Hydrogeologic Settings
- 6. Andreo B, Carrasco F, Durán J, LaMoreaux J (2010) Advances in Research in Karts Media
- 7. Andreo B, Vías J, López-Geta J, et al (2004) Propuesta metodológica para la estimación de la recarga en acuíferos carbonáticos. Bol Geol y Min 115:177–186
- 8. Aranda N, Elis VR, Prado RL, et al (2021) Electrical resistivity methods to characterize the moisture content in Brazilian sanitary landfill. Environ Monit Assess 193:1–15. https://doi.org/10.1007/S10661-021-09050-W/FIGURES/11
- 9. Aranda N, Prado RL, Elis VR, et al (2019) Evaluating elastic wave velocities in Brazilian municipal solid waste. Environ Earth Sci 78:1–16. https://doi.org/10.1007/S12665-019-8490-Y/FIGURES/16
- 10. Awawdeh M, Obeidat M, Zaiter G (2015) Groundwater vulnerability assessment in the vicinity of Ramtha wastewater treatment plant, North Jordan. Appl Water Sci 5:321–334. https://doi.org/10.1007/s13201-014-0194-6
- 11. Ayed B, Jmal I, Sahal S, et al (2017) Comparison between an intrinsic and a specific vulnerability method using a GIS tool: Case of the Smar aquifer in Maritime Djeffara (southeastern Tunisia). J Water Supply Res Technol AQUA 66:186–198. https://doi.org/10.2166/aqua.2017.081
- 12. Bakalowicz M (2019) Epikarst. In: Encyclopedia of Caves. Academic Press, pp 394–398
- 13. Baloch MA, Sahar L (2014) Development of a watershed-based geospatial groundwater specific vulnerability assessment tool. Groundwater 52:137–147. https://doi.org/10.1111/gwat.12212

- 14. Barea J, López-Martínez J, Durán JJ (2002) Desarrollo del karst versus litoestratigrafía en los bordes norte y sur del Sistema Central español. Bol Geol y Min 113:155–164
- 15. Bhuvaneswaran C, Ganesh A (2019) Spatial assessment of groundwater vulnerability using DRASTIC model with GIS in Uppar odai sub-watershed, Nandiyar, Cauvery Basin, Tamil Nadu. Groundw Sustain Dev 9:100270. https://doi.org/10.1016/j.gsd.2019.100270
- 16. Boufekane A, Saighi O (2018) Application of Groundwater Vulnerability Overlay and Index Methods to the Jijel Plain Area (Algeria). Groundwater 56:143–156. https://doi.org/10.1111/gwat.12582
- 17. Buckalew J, Scott L, James M, Reed P (1998) Evaluacion de los Recursos de Agua del Ecuador REPORT
- Cabrera M, Moulatlet GM, Valencia BG, et al (2022) Microplastics in a tropical Andean Glacier: A transportation process across the Amazon basin? Sci Total Environ 805:150334. https://doi.org/10.1016/J.SCITOTENV.2021.150334
- 19. Cabrera M, Valencia BG, Lucas-Solis O, et al (2020) A new method for microplastic sampling and isolation in mountain glaciers: A case study of one antisana glacier, Ecuadorian Andes. Case Stud Chem Environ Eng 2:100051. https://doi.org/10.1016/J.CSCEE.2020.100051
- 20. Calero JL, Conicelli B, Valencia BG (2022) Determination of an age model based on the analysis of the δ 180 cyclicity in a tropical glacier. J South Am Earth Sci 116:103808. https://doi.org/10.1016/J.JSAMES.2022.103808
- 21. Campoverde-Muñoz P, Aguilar-Salas L, Romero-Crespo P, et al (2023) Risk Assessment of Groundwater Contamination in the Gala, Tenguel, and Siete River Basins, Ponce Enriquez Mining Area—Ecuador. Sustain 15:403. https://doi.org/10.3390/su15010403
- 22. Capparelli M V., Cabrera M, Rico A, et al (2021) An Integrative Approach to Assess the Environmental Impacts of Gold Mining Contamination in the Amazon. Toxics 9:149. https://doi.org/10.3390/toxics9070149
- 23. Capparelli M V., Moulatlet GM, de Souza Abessa DM, et al (2020) An integrative approach to identify the impacts of multiple metal contamination sources on the Eastern Andean foothills of the Ecuadorian Amazonia. Sci Total Environ 709:. https://doi.org/10.1016/j.scitotenv.2019.136088
- 24. Chamba B (2020) The First Electrical Resistivity Tomography Study Applied to an Ecuadorian Cave (Uctu Iji Changa, Tena): Insights into Amazonian Karst Systems. Universidad de Investigación Experimental de Tecnología Experimental Yachay
- 25. Coello X, Galárraga R (2002) Análisis comparativo de la vulnerabilidad del acuífero norte de Quito. XII Congr Bras Águas Subterrâneas 35
- 26. Conicelli B, Hirata R, Galvão P, et al (2021) Groundwater governance: The illegality of exploitation and ways to minimize the problem. An Acad Bras Cienc 93:e20200623. https://doi.org/10.1590/0001-3765202120200623
- 27. Conicelli B, Hirata R, Galvão P, et al (2020) Determining groundwater availability and aquifer recharge using GIS in a highly urbanized watershed. J South Am Earth Sci 106:103093. https://doi.org/10.1016/j.jsames.2020.103093
- 28. Constantin S, Toulkeridis T, Moldovan OT, et al (2018) Caves and karst of Ecuador-state-of-the-art and research perspectives. Phys Geogr 40:28-51. https://doi.org/10.1080/02723646.2018.1461496
- 29. Davis AD, Long AJ, Wireman M (2002) KARSTIC: A sensitivity method for carbonate aquifers in karst terrain. Environ Geol 42:65–72. https://doi.org/10.1007/s00254-002-0531-1

- 30. de Castro T, Menegasse L (2017) Assessment of intrinsic vulnerability to the contamination of karst aquifer using the COP method in the Carste Lagoa Santa Environmental Protection Unit, Brazil. Environ Earth Sci 76:1–13. https://doi.org/10.1007/s12665-017-6760-0
- 31. Doerfliger N, Jeannin PY, Zwahlen F (1999) Water vulnerability assessment in karst environments: a new method of defining protection areas using a multi-attribute approach and GIS tools (EPIK method). Environ Geol 39:165–176. https://doi.org/10.1007/s002540050446
- 32. Doerfliger N, Zwahlen F (1998) Practical Guide Groundwater Vulnerability Mapping in Karstic Regions (EPIK). Berna, Suiza
- 33. Dos Santos Filho MG, Hirata R, Luiz MB, Conicelli B (2017) Solo e águas subterrâneas contaminadas pela deposição de resíduos sólidos urbanos: o caso do Vazadouro de Tatuí (SP). Rev do Inst Geológico 38:31–47. https://doi.org/10.5935/0100-929X.20170003
- 34. Doummar J, Margane A, Geyer T, Sauter M (2012) Protection of Jeita Spring: Vulnerability Mapping Using the COP and EPIK Methods
- 35. Duarte YA, Bautista F, Mendoza ME, Delgado C (2013) Vulnerability and risk of contamination karstic aquifers. Trop Subtrop Agroecosystems 16:243–263
- 36. Durán J, Espinoza K, Marina M, et al (2015) Hydrogeological and Environmental Investigations in Karst Systems. Hydrogeol Environ Investig Karst Syst 83–90. https://doi.org/10.1007/978-3-642-17435-3
- 37. Entezari M, Karimi H, Gholam H, Jafari M (2020) Estimation of groundwater recharge level in karstic aquifers using modified APLIS model. Arab J Geosci 13:. https://doi.org/10.1007/s12517-020-5173-7
- 38. Espol Tech EP (2014) ELABORACIÓN DEL MAPA HIDROGEOLÓGICO A ESCALA 1: 250. 000. Guayaquil
- 39. Fick SE, Hijmans RJ (2017) WorldClim 2: new 1-km spatial resolution climate surfaces for global land areas. Int J Climatol 37:4302–4315. https://doi.org/10.1002/joc.5086
- 40. Flores Y, Camacho -Christian, Miklós -Rita, et al (2020) COMPARISION OF THE GENERAL HYDROGEOLOGICAL CONDITIONS OF THE KARST WATER BODIES OF HUNGARY AND ECUADOR. Geosci Eng 8:131–153
- 41. Flores Y, Szucs P (2022) CARTOGRAPHIC DELINEATION OF KARST BODIES IN THE ECUADORIAN CARTOGRAPHIC DELINEATION OF KARST BODIES IN THE. Miskolc
- 42. Foster S, Hirata R (1988) Groundwater pollution risk assessment; a methodology using available data. https://pesquisa.bvsalud.org/portal/resource/pt/lil-146657. Accessed 11 Apr 2022
- 43. Foster S, Hirata R, Gomes D, et al (2002) Proteccion de la Calidad del Agua Subterranea
- 44. Freeze RA, Cherry JA (1979) Groundwater. Prentice-Hall, Inc
- 45. Galarza E, Cabrera M, Espinosa R, et al (2021) Assessing the Quality of Amazon Aquatic Ecosystems with Multiple Lines of Evidence: The Case of the Northeast Andean Foothills of Ecuador. Bull Environ Contam Toxicol. https://doi.org/10.1007/s00128-020-03089-0
- 46. Galarza E, Moulatlet GM, Rico A, et al (2022) Human health risk assessment of metals and metalloids in mining areas of the Northeast Andean foothills of the Ecuadorian Amazon. Integr Environ Assess Manag 00:0–1. https://doi.org/10.1002/IEAM.4698
- 47. Galvão P, Hirata R, Conicelli B (2018) Estimating groundwater recharge using GIS-based distributed water balance model in an environmental protection area in the city of Sete Lagoas (MG), Brazil. Environ Earth Sci 77:0. https://doi.org/10.1007/s12665-018-7579-z

- 48. Gogu R, Dassargues A (2000) Sensitivity analysis for the EPIK method of vulnerability assessment in a small karstic aquifer, southern Belgium. Hydrogeol J 8:337–345. https://doi.org/10.1007/s100400050019
- 49. Goldscheider N (2005) Karst groundwater vulnerability mapping: Application of a new method in the Swabian Alb, Germany. Hydrogeol J 13:555–564. https://doi.org/10.1007/s10040-003-0291-3
- 50. Hadžić E, Lazović N, Mulaomerović-Šeta A (2015) The Importance of Groundwater Vulnerability Maps in the Protection of Groundwater Sources. Key Study: Sarajevsko Polje. In: Procedia Environmental Sciences. Elsevier, pp 104–111
- 51. Hammouri N, El-Naqa A (2008) GIS based hydrogeological vulnerability mapping of groundwater resources in Jerash area Jordan. Geofis Int 47:85–87. https://doi.org/10.22201/igeof.00167169p.2008.47.2.70
- 52. Hasan M, Islam MA, Aziz Hasan M, et al (2019) Groundwater vulnerability assessment in Savar upazila of Dhaka district, Bangladesh A GIS-based DRASTIC modeling. Groundw Sustain Dev 9:100220. https://doi.org/10.1016/j.gsd.2019.100220
- 53. Hirata R, Conicelli BP (2012) Groundwater resources in Brazil: A review of possible impacts caused by climate change. An Acad Bras Cienc 84:297–312. https://doi.org/10.1590/S0001-37652012005000037
- 54. Hurtado-Pidal J, Acero Triana JS, Aguayo M, et al (2022) Is forest location more important than forest fragmentation for flood regulation? Ecol Eng 183:106764. https://doi.org/10.1016/J.ECOLENG.2022.106764
- 55. INAMHI (2013) Mapa de Isoyetas media anual / Serie 81-2010. Quito, Ecuador
- 56. Intriago A, Galvão P, Conicelli B (2023) Use of GIS and R to estimate climate change impacts on groundwater recharge in Portoviejo River watershed, Ecuador. J South Am Earth Sci 124:104288. https://doi.org/10.1016/J.JSAMES.2023.104288
- 57. Jang WS, Engel B, Harbor J, Theller L (2017) Aquifer vulnerability assessment for sustainable groundwater management using DRASTIC. Water (Switzerland) 9:. https://doi.org/10.3390/w9100792
- 58. Jarrín AE, Salazar JG, Martínez-Fresneda Mestre M (2017) Evaluación del riesgo a la contaminación de los acuíferos de la Reserva Biológica de Limoncocha, Amazonía Ecuatoriana. Rev Ambient e Água 12:652–665. https://doi.org/10.4136/1980-993X
- 59. Jiménez-Iñiguez A, Ampuero A, Valencia BG, et al (2022) Stable isotope variability of precipitation and cave drip-water at Jumandy cave, western Amazon River basin (Ecuador). J Hydrol 610:127848. https://doi.org/10.1016/J.JHYDROL.2022.127848
- 60. Jiménez-Madrid A, Gogu R, Martinez-Navarrete C, Carrasco F (2019) Groundwater for human consumption in karst environment: Vulnerability, protection, and management. Handb Environ Chem 68:45–63. https://doi.org/10.1007/978-3-319-77368-1\_2
- 61. Khan R, Jhariya DC (2019) Assessment of Groundwater Pollution Vulnerability Using GIS Based Modified DRASTIC Model in Raipur City, Chhattisgarh. J Geol Soc India 93:293–304. https://doi.org/10.1007/s12594-019-1177-x
- 62. Khosravi K, Sartaj M, Tsai FTC, et al (2018) A comparison study of DRASTIC methods with various objective methods for groundwater vulnerability assessment. Sci Total Environ 642:1032–1049. https://doi.org/10.1016/j.scitotenv.2018.06.130
- 63. Kumar A, Krishna AP (2020) Groundwater vulnerability and contamination risk assessment using GIS-based modified DRASTIC-LU model in hard rock aquifer system in India. Geocarto Int 35:1149–1178. https://doi.org/10.1080/10106049.2018.1557259

- 64. Lenhare BD, Sallun Filho W (2019) Application of EPIK and KDI methods for identification and evaluation of karst vulnerability at Intervales State Park and surrounding region (Southeastern Brazil). Carbonates and Evaporites 34:175–187. https://doi.org/10.1007/s13146-018-0474-6
- 65. Lerner DN, Harris B (2009) The relationship between land use and groundwater resources and quality. Land use policy 26:265–273. https://doi.org/10.1016/j.landusepol.2009.09.005
- 66. Lessmann J, Fajardo J, Muñoz J, Bonaccorso E (2016) Large expansion of oil industry in the Ecuadorian Amazon: biodiversity vulnerability and conservation alternatives. Ecol Evol 6:4997–5012. https://doi.org/10.1002/ece3.2099
- 67. Lodwick WA, Monson W, Svoboda L (1990) Attribute error and sensitivity analysis of map operations in geographical informations systems: Suitability analysis. Int J Geogr Inf Syst 4:413–428. https://doi.org/10.1080/02693799008941556
- 68. Lucas-Solis O, Moulatlet GM, Guamangallo J, et al (2021) Preliminary Assessment of Plastic Litter and Microplastic Contamination in Freshwater Depositional Areas: The Case Study of Puerto Misahualli, Ecuadorian Amazonia. Bull Environ Contam Toxicol. https://doi.org/10.1007/s00128-021-03138-2
- 69. MAGAP (2015) Manual de Procedimientos de Geopedología. Quito, Ecuador
- 70. Majandang J, Sarapirome S (2013) Groundwater vulnerability assessment and sensitivity analysis in Nong Rua, Khon Kaen, Thailand, using a GIS-based SINTACS model. Environ Earth Sci 68:2025–2039. https://doi.org/10.1007/s12665-012-1890-x
- 71. Maqsoom A, Aslam B, Khalil U, et al (2020) A GIS-based DRASTIC Model and an Adjusted DRASTIC Model (DRASTICA) for Groundwater Susceptibility Assessment along the China-Pakistan Economic Corridor (CPEC) Route. ISPRS Int J Geo-Information 9:. https://doi.org/10.3390/ijgi9050332
- 72. Marín Al, Andreo B (2015) Vulnerability to Contamination of Karst Aquifers. In: Stevanović Z (ed) Karst Aquifers Characterization and Engineering. p 698
- 73. Merchán P, Chiogna G (2017) Assessment of contamination by petroleum hydrocarbons from oil exploration and production activities in Aquarico, Ecuador. Munich, Germany
- 74. Moustafa M (2019) Assessing perched aquifer vulnerability using modified DRASTIC: a case study of colliery waste in north-east England (UK). Hydrogeol J 27:1837–1850. https://doi.org/10.1007/s10040-019-01932-1
- 75. Napolitano P, Fabbri AG (1996) Single-parameter sensitivity analysis for aquifer vulnerability assessment using DRASTIC and SINTACS. In: HydroGIS 96: Application of Geographic Information Systems in Hydrology and Water Resources Management (Proceedings of the Vienna Conference, April 1996). pp 559–566
- 76. Nekkoub A, Baali F, Hadji R, Hamed Y (2020) The EPIK multi-attribute method for intrinsic vulnerability assessment of karstic aquifer under semi-arid climatic conditions, case of Cheria Plateau, NE Algeria. Arab J Geosci 13:. https://doi.org/10.1007/s12517-020-05704-0
- 77. Oke SA (2020) Regional aquifer vulnerability and pollution sensitivity analysis of drastic application to dahomey basin of Nigeria. Int J Environ Res Public Health 17:. https://doi.org/10.3390/ijerph17072609
- 78. Oroji B, Karimi ZF (2018) Application of DRASTIC model and GIS for evaluation of aquifer vulnerability: case study of Asadabad, Hamadan (western Iran). Geosci J 22:843–855. https://doi.org/10.1007/s12303-017-0082-9
- 79. Ouedraogo I, Defourny P, Vanclooster M (2016) Mapping the groundwater vulnerability for pollution at the pan African scale. Sci Total Environ 544:939–953. https://doi.org/10.1016/j.scitotenv.2015.11.135

- 80. Pacheco R, Pacheco J, Ye M, Cabrera A (2018) Groundwater Quality: Analysis of Its Temporal and Spatial Variability in a Karst Aguifer. Groundwater 56:62–72. https://doi.org/10.1111/gwat.12546
- 81. Pathak DR, Hiratsuka A, Awata I, Chen L (2009) Groundwater vulnerability assessment in shallow aquifer of Kathmandu Valley using GIS-based DRASTIC model. Environ Geol 57:1569–1578. https://doi.org/10.1007/s00254-008-1432-8
- 82. Peñafiel L, Alcalá FJ, Senent-Aparicio J (2021) Usefulness of Compiled Geophysical Prospecting Surveys in Groundwater Research in the Metropolitan District of Quito in Northern Ecuador. Appl Sci 2021, Vol 11, Page 11144 11:11144. https://doi.org/10.3390/APP112311144
- 83. Pereira DL, Galvão P, Lucon T, Fujaco MA (2019) Adapting the EPIK method to Brazilian Hydro(geo)logical context of the São Miguel watershed to assess karstic aquifer vulnerability to contamination. J South Am Earth Sci 90:191–203. https://doi.org/10.1016/j.jsames.2018.12.011
- 84. Pileggi F, Hirata R, Aranda N, Conicelli B (2021) Support method for interpretation of regional groundwater monitoring in urban areas. Brazilian J Geol 51:e20200053. https://doi.org/10.1590/2317-4889202120200053
- 85. Pimm SL, Jenkins CN, Abell R, et al (2014) The biodiversity of species and their rates of extinction, distribution, and protection. Science (80-) 344:. https://doi.org/10.1126/SCIENCE.1246752
- 86. Ramaraju A V, Krishna Veni K (2017) Groundwater vulnerability Assessment by DRASTIC method using GIS. SSRG Int J Geo informatics Geol Sci 4:1–8
- 87. Ravbar N, Goldscheider N (2009) Comparative application of four methods of groundwater vulnerability mapping in a Slovene karst catchment. Hydrogeol J 17:725–733. https://doi.org/10.1007/s10040-008-0368-0
- 88. Ribeiro L, Pindo JC, Dominguez-Granda L (2017) Assessment of groundwater vulnerability in the Daule aquifer, Ecuador, using the susceptibility index method. Sci Total Environ 574:1674–1683. https://doi.org/10.1016/J.SCITOTENV.2016.09.004
- 89. Sahoo S, Dhar A, Kar A, Chakraborty D (2016) Index-based groundwater vulnerability mapping using quantitative parameters. Environ Earth Sci 75:. https://doi.org/10.1007/s12665-016-5395-x
- 90. Saida S, Tarik H, Abdellah A, et al (2017) Assessment of groundwater vulnerability to nitrate based on the optimised DRASTIC models in the GIS environment (Case of sidi rached basin, Algeria). Geosci 7:. https://doi.org/10.3390/geosciences7020020
- 91. Saidi S, Bouri S, Ben Dhia H, Anselme B (2011) Assessment of groundwater risk using intrinsic vulnerability and hazard mapping: Application to Souassi aquifer, Tunisian Sahel. Agric Water Manag 98:1671–1682. https://doi.org/10.1016/J.AGWAT.2011.06.005
- 92. Saidi S, Bouri S, Dhia H Ben (2010) Groundwater vulnerability and risk mapping of the hajeb-jelma aquifer (central tunisia) using a gis-based drastic model. Environ Earth Sci 59:1579–1588. https://doi.org/10.1007/s12665-009-0143-0
- 93. Sanchez-Cortez JL, Jaque-Bonilla D, Simbaña-Tasiguano M, et al (2022) Participatory strategies applied for the geoconservation of speleological heritage at the Napo Sumaco Geopark (Ecuador). Episodes J Int Geosci 45:417–429. https://doi.org/10.18814/EPIIUGS/2022/022001
- 94. Sánchez Cortez JL (ed) (2017) Guía Espeleológica de la Provincia Napo. Gobierno Autónomo Descentralizado de la Provincia de Napo, Universidad Regional Amazónica IKIAM, Sociedad Científica Espeleológica Ecuatoriana (ECUACAVE), Geoparque Napo-Sumaco, Tena, Ecuador

- 95. Shirazi SM, Imran HM, Akib S, et al (2013) Groundwater vulnerability assessment in the Melaka State of Malaysia using DRASTIC and GIS techniques. Environ Earth Sci 70:2293–2304. https://doi.org/10.1007/s12665-013-2360-9
- 96. SIGTIERRAS (2015) Geomorfología. Quito, Ecuador
- 97. Stevanović Z (2015) Chap. 3: Characterization of Karst Aquifer
- 98. Talozi SA, Hijazi H (2013) Groundwater Contamination Hazards, Vulnerability and Risk GIS Mapping for Seven Municipalities in the Jordan Valley. Amman, Jordan
- 99. Terada R, Hirata R, Galvão P, et al (2022) Hydraulic relationship between aquifer and pond under potential influence of eucalyptus and sugarcane in tropical region of São Paulo, Brazil. Environ Earth Sci 81:1–16. https://doi.org/10.1007/S12665-022-10349-1/METRICS
- 100. Thapa R, Gupta S, Guin S, Kaur H (2018) Sensitivity analysis and mapping the potential groundwater vulnerability zones in Birbhum district, India: A comparative approach between vulnerability models. Water Sci 32:44–66. https://doi.org/10.1016/j.wsj.2018.02.003
- 101. Tomer T, Katyal D, Joshi V (2019) Sensitivity analysis of groundwater vulnerability using DRASTIC method: A case study of National Capital Territory, Delhi, India. Groundw Sustain Dev 9:100271. https://doi.org/10.1016/j.gsd.2019.100271
- 102. Tziritis E, Lombardo L (2017) Estimation of intrinsic aquifer vulnerability with index-overlay and statistical methods: the case of eastern Kopaida, central Greece. Appl Water Sci 7:2215–2229. https://doi.org/10.1007/s13201-016-0397-0
- 103. Umar R, Ahmed I, Alam F (2009) Mapping groundwater vulnerable zones using modified DRASTIC approach of an alluvial aquifer in parts of central Ganga plain, western Uttar Pradesh. J Geol Soc India 73:193–201. https://doi.org/10.1007/s12594-009-0075-z
- 104. V. Capparelli M, Cabrera M, Rico A, et al (2021) An Integrative Approach to Assess the Environmental Impacts of Gold Mining An integrative approach to assess the environmental impacts of gold mining contamination in the Amazon. Toxics 9:1–14. https://doi.org/10.3390/toxics9070149
- 105. Vera D, Simbaña-Tasiguano M, Guzmán O, et al (2023) Quantitative Assessment of Geodiversity in Ecuadorian Amazon—Case Study: Napo Sumaco Aspiring UNESCO Geopark. Geoheritage 15:1–14. https://doi.org/10.1007/S12371-023-00792-2/FIGURES/5
- 106. Villacís M, Vimeux F, Taupin JD (2008) Analysis of the climate controls on the isotopic composition of precipitation (δ180) at Nuevo Rocafuerte, 74.5°W, 0.9°S, 250 m, Ecuador. Comptes Rendus Geosci 340:1–9. https://doi.org/10.1016/J.CRTE.2007.11.003
- 107. Vogelbacher A, Kazakis N, Voudouris K, Bold S (2019) Groundwater vulnerability and risk assessment in a karst aquifer of Greece using EPIK method. Environ MDPI 6:1–16. https://doi.org/10.3390/environments6110116
- 108. Wei A, Bi P, Guo J, et al (2021) Modified DRASTIC model for groundwater vulnerability to nitrate contamination in the Dagujia River Basin, China. Water Supply 1–13. https://doi.org/10.2166/ws.2021.018
- 109. Zagana E, Tserolas P, Floros G, et al (2011) First outcomes from groundwater recharge estimation in evaporite aquifer in Grece with the use of APLIS method. Adv Res Aquat Environ 2:89–96. https://doi.org/10.1007/978-3-642-24076-8
- 110. Zghibi A, Merzougui A, Chenini I, et al (2016) Groundwater vulnerability analysis of Tunisian coastal aquifer: An application of DRASTIC index method in GIS environment. Groundw Sustain Dev 2–3:169–181.

111. Zwahlen F (2003) Vulnerability and Risk Mapping for the Protection of Carbonate (Karst) Aquifers. Belgium

### **Figures**

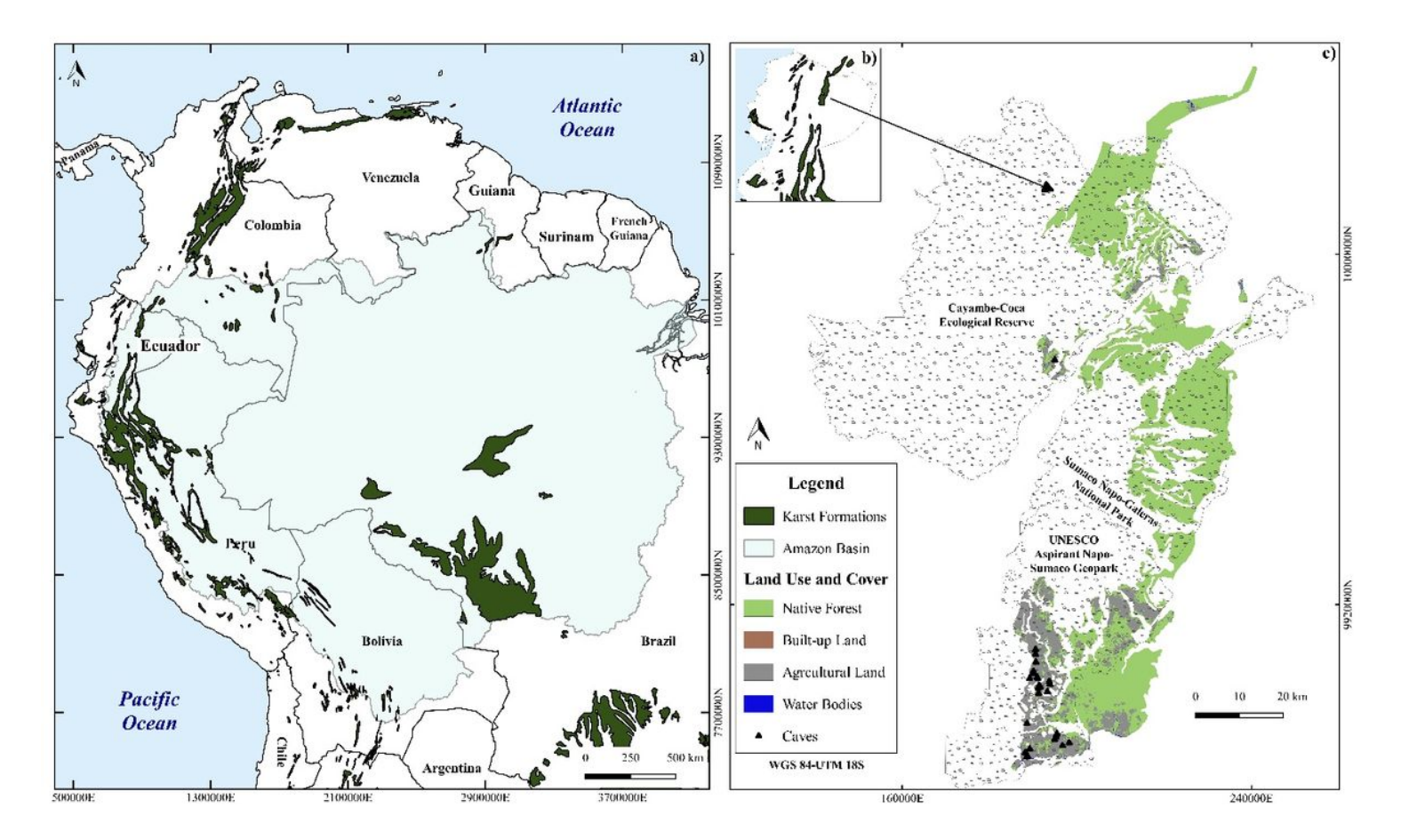


Figure 1

Geographical location of the study area. a) Karst Formations in South America and the Amazon Basin, b) Napo Karst Formation (NKF), the study area in Ecuador, c) Protected areas, Land Use and Cover, and Caves in the NKF.

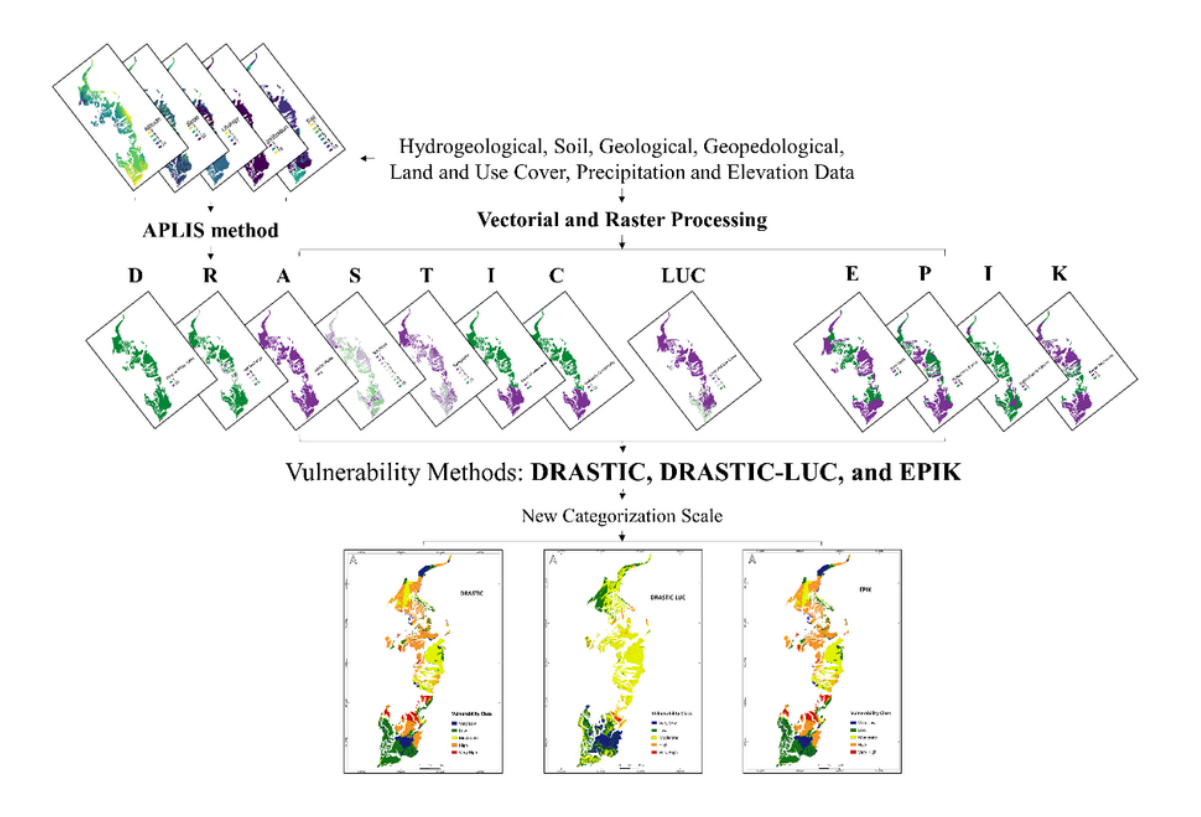


Figure 2

Flowchart of the overall methodology. We first downloaded data from the available repositories as vector or raster files. After processing, the information was inserted in the DRASTIC, DRASTIC-LUC, and EPIK models. The outcomes were vulnerability models that were further tested with sensitivity analysis.

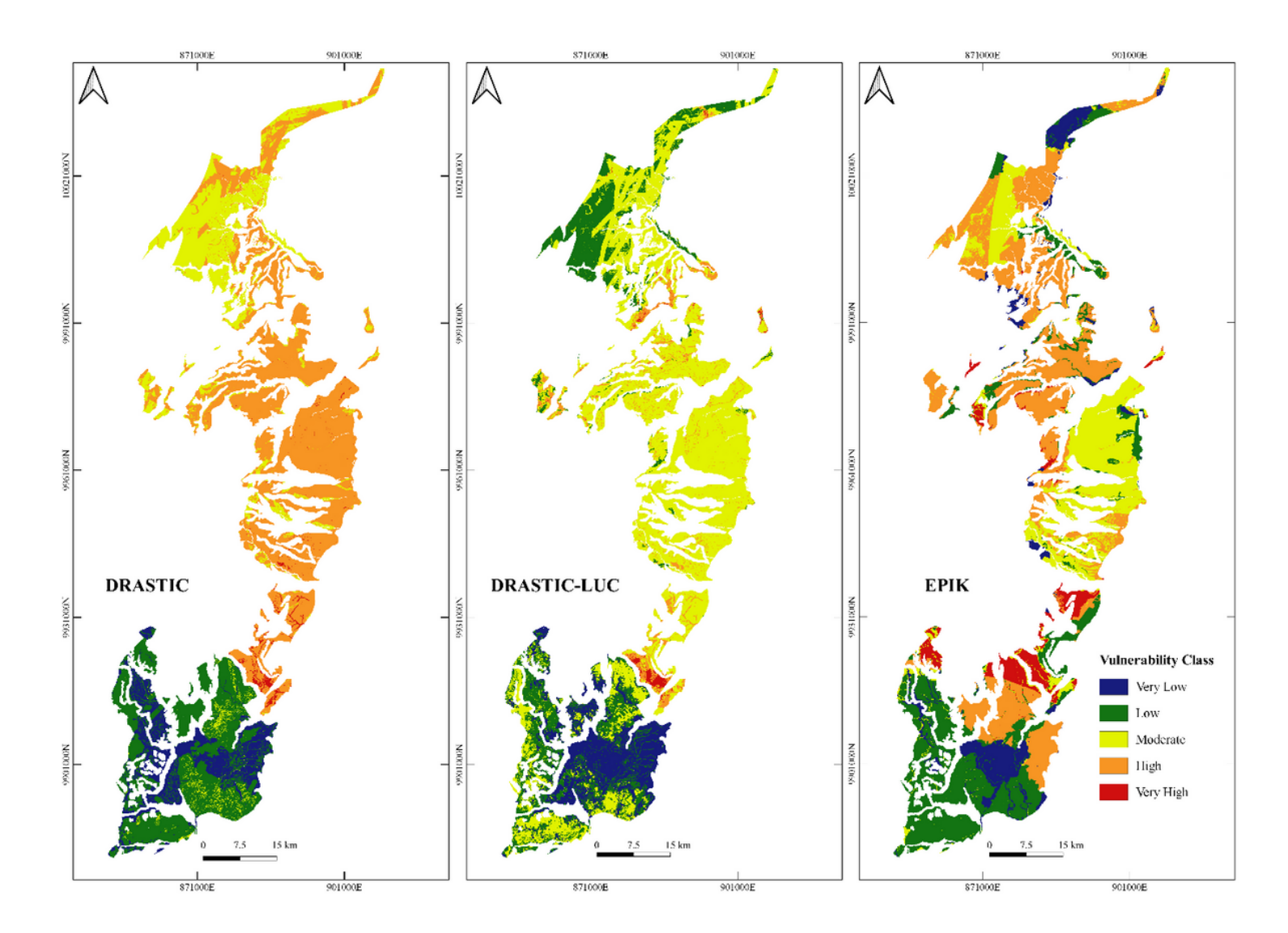
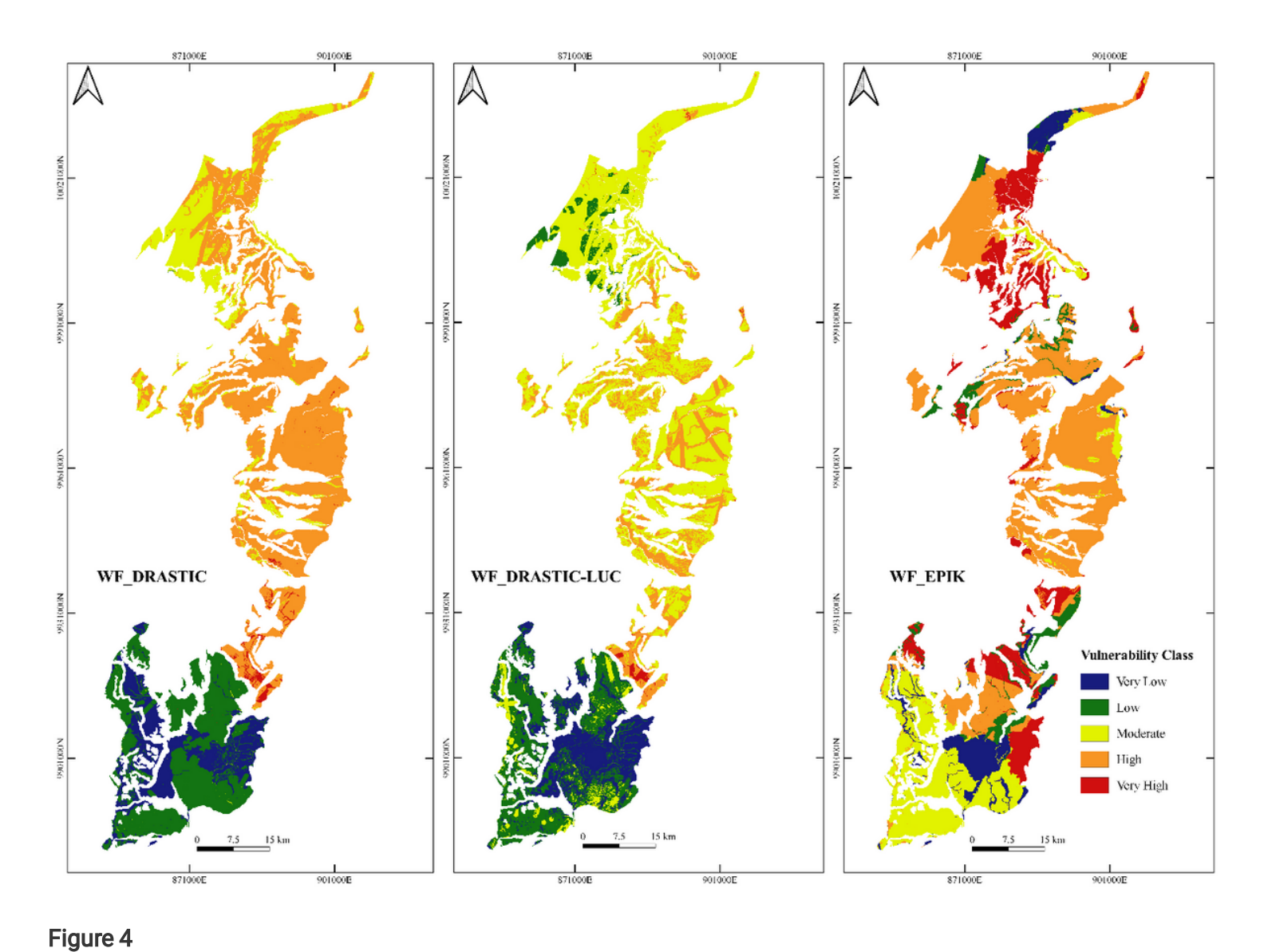


Figure 3

Vulnerability maps developed for each methodology.



Vulnerability maps after calculating the weighting factor.

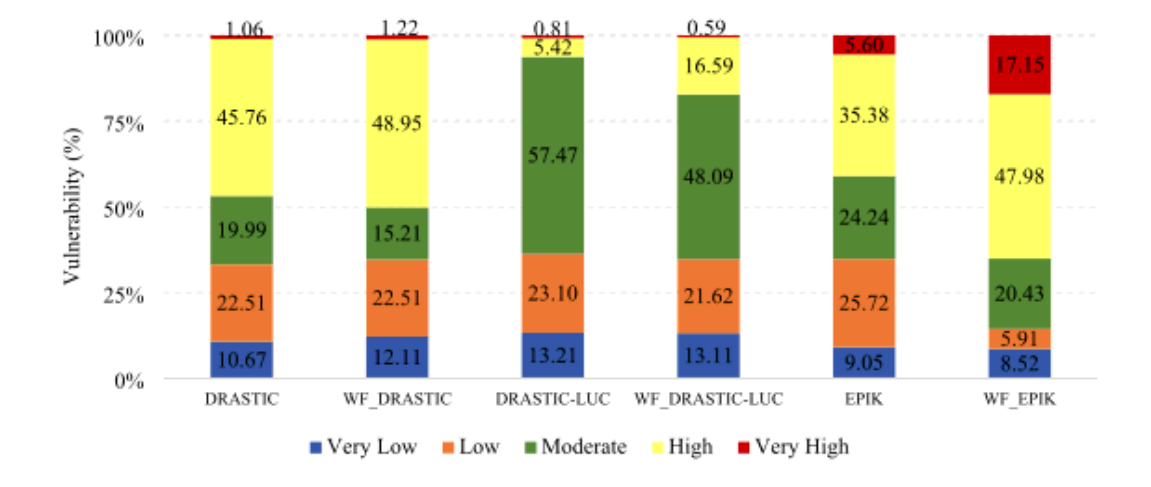


Figure 5

Area distribution in percentage for each vulnerability index after weighting factor.